LATE JURASSIC-EARLY CRETACEOUS TIME SCALES AND OCEANIC MAGNETIC ANOMALY BLOCK MODELS

JAMES E. T. CHANNELL
Department of Geology, University of Florida, Gainesville, FL 32611
ELISABETTA ERBA
Dipartimento di Scienze della Terra, Università di Milano, 20133 Milano, Italy
MASAO NAKANISHI
Ocean Research Institute, University of Tokyo, Tokyo 164, Japan and Scripps Institution of Oceanography, La Jolla, CA 92092
AND
KENSAKU TAMAKI
Ocean Research Institute, University of Tokyo, Tokyo 164, Japan

ABSTRACT: Comparison of oceanic anomaly block models in the M0-M29 interval from the Japanese, Phoenix, Hawaiian and Keathley lineations indicates that the Hawaiian block model represents the closest approximation to a constant spreading rate record. The new Hawaiian block model differs slightly from that of Larson and Hilde (1975). Currently popular numerical age estimates for polarity chrons, base CM0 (121 Ma), CM16-CM15 (137 Ma) and top CM25 (154 Ma), are consistent with constant spreading rate in the new Hawaiian block model but inconsistent with constant spreading in the Larson and Hilde (1975) block model. A new time scale (CENT94) is based on the above ages and constant spreading in the new Hawaiian block model.

Land section magnetostratigraphy, mainly from Italy and Spain, has provided direct correlations of polarity chrons to stage boundaries through ammonite biozones, and indirect correlation through nannofossil and calpionellid biozonations: Barremian-Aptian (base of CM0), Hauterivian-Barremian (upper part of CM4), Valanginian-Hauterivian (base of CM11n), Berriasian-Valanginian (CM15n), Tithonian-Berriasian (base of CM18), Kimmeridgian-Tithonian (CM22A) and Oxfordian-Kimmeridgian (top CM25). These correlations yield the following stage boundary ages using CENT94: Barremian-Aptian (121 Ma), Hauterivian-Barremian (126 Ma), Valanginian-Hauterivian (131.5 Ma), Berriasian-Valanginian (135.8 Ma), Tithonian-Berriasian (141.6 Ma), Kimmeridgian-Tithonian (150 Ma), and Oxfordian-Kimmeridgian (154 Ma).

INTRODUCTION

The Late Jurassic-Early Cretaceous time scales of Kent and Gradstein (1985, KG85) and Harland and others (1990, GTS89) imply constant spreading rate in the M0-M25 Hawaiian oceanic anomaly block model of Larson and Hilde (1975, LH75). The KG85 time scale uses the constant spreading rate assumption to interpolate between 119 Ma for the Barremian-Aptian boundary (base CM0*) and 156 Ma for the Oxfordian-Kimmeridgian boundary (CM25n). The GTS89 time scale is based on chronogram ages for the Late Jurassic-Early Cretaceous stage boundaries. These ages were used to make a linear recalibration of the KG85 time scale, thereby inheriting the constant spreading rate assumption. The chronograms of GTS89 for this interval are poorly constrained and therefore do little to validate the constant spreading rate assumption.

Gradstein and others (1994, this volume) have presented integrated Triassic to Cretaceous time scales. GRAD94 supersedes an earlier version (GRAD93) presented at the AAPG/SEPM special symposium in New Orleans in April, 1993. In both time scales, radiometric ages were used to construct maximum likelihood chronograms for stage boundary ages. The maximum likelihood age estimates were then combined (weighted average) with stage boundary age estimates from magnetochronology. The magnetochronological estimates utilize magnetostratigraphic correlations of polarity chrons to stage boundaries, and the LH75 constant spreading rate block model to interpolate between polarity chron ages. For GRAD93, the magnetochronological interpolation is among five polarity chron age estimates: CM0 base (122 Ma), CM10N base (130 Ma), CM16n (137 Ma), CM21n base (145 Ma) and CM25n top (154 Ma). The GRAD93 time scale ages differ significantly from these magnetochronological tie-point ages, due to the weighting of the radiometric chronogram estimates which incorporate both high and low temperature radiometric ages. For GRAD94, the magnetochronological LH75 interpolation is between two ages: CM1 top (at 123.5 Ma) and CM26 (at 155.3 Ma), and radiometric control is restricted to high temperature ages.

Obradovich (1993) presented a Cretaceous time scale (OBRAD93) in which the Early Cretaceous portion is based on constant, but different, spreading rates for two intervals of LH75 defined by three age tie points: CM0 at 121 Ma, CM16/CM16n at 137 Ma and CM25n at 156 Ma. The resulting time scale implies a spreading rate change in LH75 at CM16/CM16n.

In this paper, we present block models derived from the Japanese, Hawaiian and Phoenix magnetic anomaly lineations, and compare these models with published data from the Hawaiian and Keathley lineations (Larson and Hilde, 1975; Klitgord and Schouten, 1986). The availability of block models from different seafloor spreading centers allows apparent spreading rate changes to be assessed and provides an independent means of evaluating time scales.

OCEANIC ANOMALY BLOCK MODELS

The Japanese, Hawaiian and Phoenix block models are based on selected magnetic anomaly profiles (Table 1, Fig. 1) from the cruise data used by Nakanishi and others (1989, 1992). For each lineation set (Fig. 2), the linkage between individual profiles was based on matching overlapping profile segments. Each selected profile was projected perpendicular to the local strike of the magnetic anomaly lineation using Generic Mapping Tools (GMT, Wessel and Smith, 1991). Inverse earth and phase filters (Schouten and McCamy, 1972) were applied to each profile, and profiles were filtered to remove the short and long wavelength components. Reversal boundaries between the prin-

*polarity chron nomenclature after Harland and others (1982, p. 80–82) with the prefix "C" to distinguish polarity chrons from oceanic magnetic anomalies

Geochronology: Time Scales and Global Stratigraphic Correlation, SEPM Special Publication No. 54
[illegible] 1995, SEPM (Society for Sedimentary Geology), ISBN 1-56576-024-7

TABLE 1.—CRUISE PROFILES USED TO CONSTRUCT OCEANIC MAGNETIC ANOMALY BLOCK MODELS (SEE NAKANISHI AND OTHERS, 1989, 1992, FOR COMPLETE LIST OF CRUISE PROFILES FROM WHICH CHOICE WAS MADE).

Japanese	Phoenix	Hawaiian
ZTES03AR (M1–M3)	7TOW3BWT (M1–M4)	POL7201 (M0–M29)
V2006 (M4–M10)	GH7801 (M5–M11)	
V3212 (M10N–M16)	C1205 (M12–M17)	
V3214 (M17–M21)	V3214 (M18–M29)	
JPYN04BD (M22–M27)		
KH87-3 (M28–M29)		

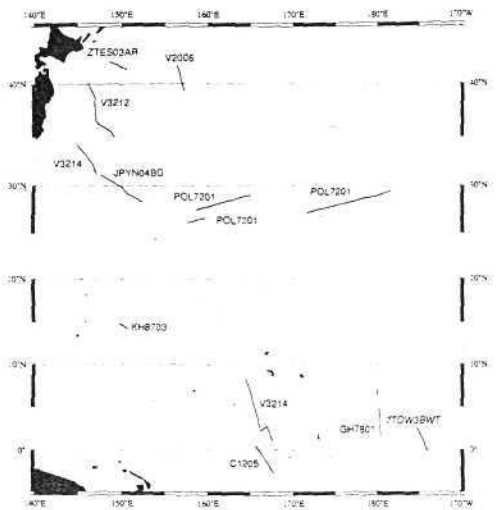

FIG. 1.—Location of track lines used to construct the block models for this study.

cipal magnetic anomalies were determined on the basis of local zero crossings (see example in Fig. 3). In a few cases, the procedure did not produce a zero crossing for a major anomaly, and reversal boundaries had to be estimated by eye. The method is more objective than picking anomaly boundaries by eye, but has the disadvantage that short wavelength minor anomalies are obscured by the filtering procedure. We therefore consider only the major anomaly boundaries (Fig. 4, Table 2). No attempt was made to place reversals associated with small amplitude anomalies in the block models. The distance data for the Keathley record (Table 2) are based on spreading rates from Klitgord and Schouten (1986).

The distances between reversals in the Japanese, Hawaiian and Phoenix block models can now be compared with one another, and with LH75 and the Keathley block model. The Phoenix block model reveals the most variable spreading rate. The similarity in shape of the plot of the Japanese, Hawaiian and Keathley block model distances against the Phoenix block model distances (Fig. 5) indicates that the spreading rate changes are predominantly in the Phoenix record. The plot of the Japanese and Hawaiian block models against the Keathley record (Fig. 6) indicates a spreading rate change at M21 which is most likely to be a change in the Keathley spreading rate rather than in the Japanese, Hawaiian and LH75 block models (see also Sundvik and Larson, 1988). The Hawaiian block model differs slightly from LH75 as illustrated by the gradual inflexion in the plot of these two block models at about M16 time (Fig. 7). This slight inflexion at about M16 time is also seen in the plot of the LH75 record against the Japanese and Keathley records (Fig. 7), and therefore, is probably an artifact of LH75.

The POL7201 tracks used as the basis for our Hawaiian block model (Figs. 1, 2; Table 1) are part of the NOAA1-4 tracks used as the basis for LH75. We attribute the differences between the new Hawaiian block model and LH75 to different emphasis given to the various tracks in constructing the block models, and to different methods used in picking anomaly boundaries and in splicing of profiles across the Waghenaer (Mendocino) fracture zones.

SELECTION OF ABSOLUTE AGES FOR A REVISED TIME SCALE

Mahoney and others (1993) obtained a $^{40}Ar/^{39}Ar$ age of 122.3 ± 1 Ma for the basaltic basement at ODP Site 807 on the Ontong Java Plateau. Tarduno and others (1991) have argued that Ontong Java volcanism is constrained to a short Early Aptian interval. This interpretation was based on the observation that sediments overlying basaltic basement, and volcanoclastic sediments at distal sites, belong to the *Globigerinelloides blowi* planktonic foraminiferal zone, which was considered to be confined to the Early Aptian interval (Sliter, 1992). Recent Lower Cretaceous planktonic foraminiferal biostratigraphy in sections dated with ammonites and magnetostratigraphy (Coccioni and others, 1992) has indicated that the *G. blowi* Zone extends into the Barremian stage (see Fig. 8). The first occurrence (FO) of *G. blowi* has now been correlated to the upper part of CM3 (middle Barremian) and the presence of the *G. blowi* Biozone does not, therefore, restrict Ontong Java volcanism to the Early Aptian interval. In the standard low-latitude nannofossil biozonation of Thierstein (1971, 1973, 1976), two zones were identified in the Aptian (Fig. 8). The base of the *Chiastozygus litterarius* Zone was identified by the FO of *C. litterarius*, the FO of *Rucinolithus irregularis* and the last occurrence (LO) of *Nannoconus colomii*. Recent biostratigraphic studies (Coccioni and others, 1992; Erba, in prep.) have shown that of these three events only the FO of *R. irregularis* is a reliable marker for the base of this zone (Fig. 8). In Thierstein's zonation, the base of the *Rhagodiscus angustus* Zone was defined by the FO of *R. angustus* and the FO of *Eprolithus floralis*. Recent biostratigraphic studies have confirmed that the FO of *E. floralis* is reliable, being consistently correlative to the base of the *L. cabri* foraminiferal Zone, whereas *R. angustus* often occurs in the underlying *C. litterarius* Zone and *G. blowi* Zone (Larson and others, 1993; Fig. 8). At Site 807 on the Ontong Java Plateau, the oldest sediments above basement can be attributed to the *C. litterarius* Zone based on the FO of *R. irregularis*. Moreover, they correlate to the upper part of this biozone, above the "nannoconid crisis" which is a distinct nannofossil event occurring post CM0 (Erba, in prep.; Fig. 8). The $^{40}Ar/^{39}Ar$ age of 122.3 ± 1 Ma for the basaltic basement at this site (Mahoney and others, 1993) obviously predates these sediments.

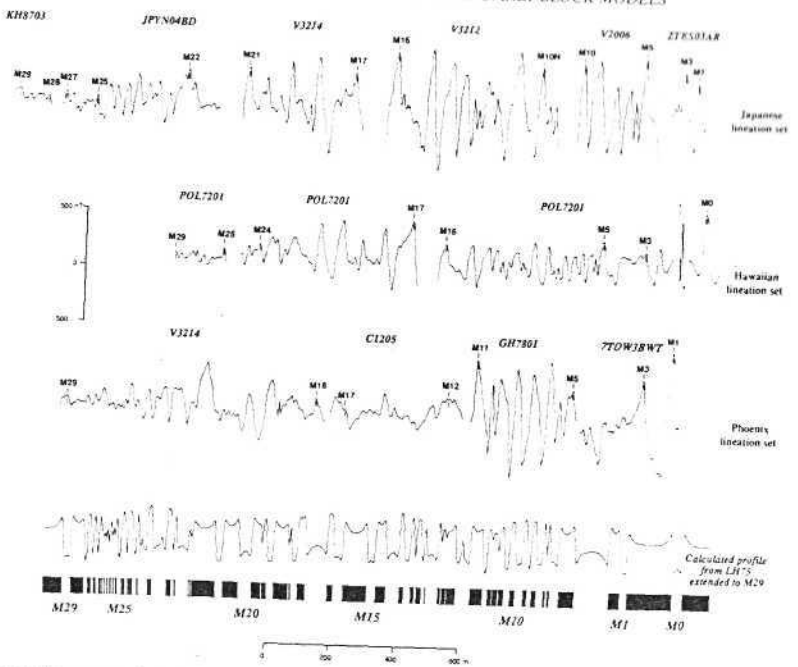

FIG. 2.—Profiles used to construct the block models. The calculated profile is the simulation from the Larson and Hilde (1975) block model extended to M29.

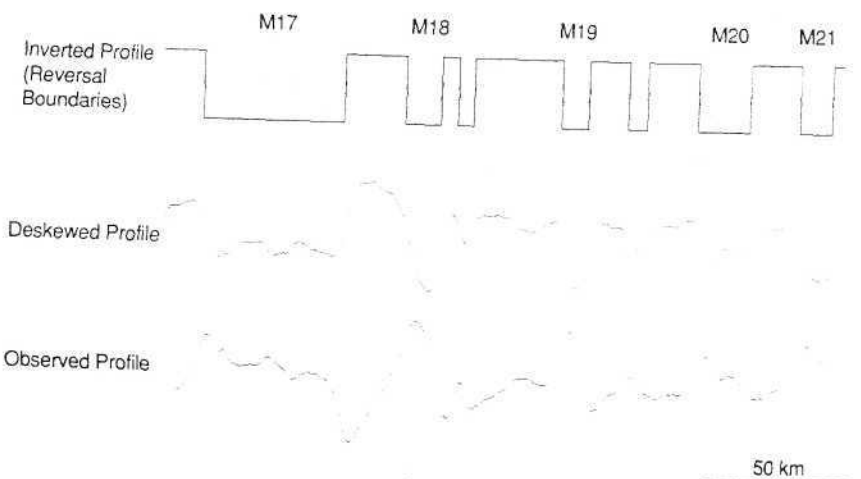

FIG. 3.—An example of the analytical procedure, illustrated using part of the profile from V3214 (Japanese lineations).

FIG. 4.—Comparison of Japanese, Phoenix, new Hawaiian and Larson and Hilde (1975) (Hawaiian) block models.

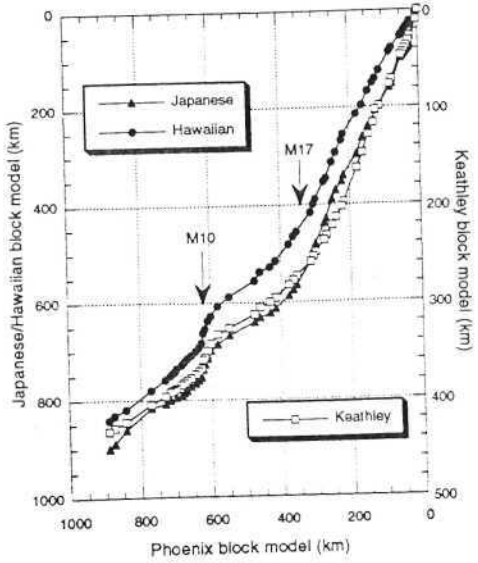

FIG. 5.—Block model distances for Japanese-Hawaiian-Keathley lineations plotted against Phoenix block model distances.

At Site 878 on MIT Guyot, the oldest dated sediments (at 25m above basement) are from the lower part of the *C. litterarius* nannofossil Zone, based on the FO of *R. irregularis* and their location below the "nannoconid crisis" (Erba and others, in prep.). Pringle and others (1993) obtained a $^{40}Ar/^{39}Ar$ age of 121.8 ± 0.5 Ma from these basalts. The standard used by Pringle and others (1993) (MMhb-1 513.9 Ma) is different from that used by Mahoney and others (1993; MMhb-1 520.4 Ma), therefore the $^{40}Ar/^{39}Ar$ ages at the two sites cannot be directly compared. Applying the conversion factor (*1.01417) to the age obtained by Pringle and others (1993) from the MIT Guyot, we obtain an age of 123.5 ± 0.5 Ma (Pringle, pers. commun., 1993). The remanent magnetization in the basaltic basement indicates a reversed polarity zone overlying a normal polarity zone (Nakanishi and Gee, in prep.; Fig. 8). The reversed polarity zone may be correlative to CM0 or CM1, however, in view of the earliest Aptian age of sediments located 25 m above basement, we correlate the reversed polarity zone to CM1.

Coleman and Bralower (1993) obtained a U-Pb zircon age of 122 ± 0.3 Ma from a bentonite in the Great Valley Group (Northern California). This level has been correlated to the *C. litterarius* Zone based on the FO of *C. litterarius*. Unfortunately, *R. irregularis* has not been found in the section (Bralower, pers. commun., 1993). As discussed above, *C. litterarius* has been reported from several Barremian sections and cannot, therefore, be used to define the Barremian/Aptian boundary, and the 122 ± 0.3 Ma bentonite layer from the Great Valley Group may be Barremian.

TABLE 2.—BLOCK MODEL DISTANCES FOR JAPANESE, PHOENIX, HAWAIIAN AND KEATHLEY BLOCK MODELS. KEATHLEY DATA AFTER KLITGORD AND SCHOUTEN (1986).

Anomaly	Japanese (km)	Phoenix (km)	Hawaiian (km)	Keathley (km)
M0			904.125	461.361
			894.317	455.971
M1	899.962	891.679	840.710	432.024
	889.484	874.779	831.878	428.636
M3	860.998	842.187	819.704	422.630
	816.742	770.319	780.132	404.689
M5	808.158	730.382	758.022	396.142
	800.642	716.484	749.639	391.676
M6		704.612	744.905	390.444
		709.693	741.760	389.443
M7	795.222	698.741	735.535	388.057
	790.992	685.407	728.085	384.592
M8	785.415	677.625	721.222	381.820
	780.724	669.519	714.643	379.741
M9	772.382	657.244	707.912	377.354
	765.783	644.258	700.255	373.350
M10	759.656	635.594	692.277	370.347
	753.641	628.089	683.139	367.498
M10N	736.367	622.042	662.104	358.489
	726.183	616.665	653.439	356.256
M11	714.193	609.815	637.234	349.480
	697.508	600.153	627.371	342.011
M12	685.752	580.878	606.520	332.386
	667.295	547.587	588.169	326.149
M13	656.820		569.502	317.833
	649.101		563.041	314.291
M14	640.983	476.678	556.149	312.058
	631.128	460.983	537.733	305.051
M15	622.379	432.058	528.053	299.584
	612.653	416.286	515.153	295.195
M16	587.276	378.327	481.845	282.182
	575.722	364.615	465.852	277.716
M17	565.080	354.385	456.384	273.516
	515.423	314.054	416.824	258.616
M18	493.424	307.036	399.402	252.916
	480.920	300.691	389.178	248.716
M19	437.869	275.552	354.056	236.416
	428.366	269.072	346.919	231.816
M20	389.600	251.352	314.145	221.516
	371.087	240.451	294.031	212.916
M21	353.017	223.436	268.698	202.016
	341.516	218.444	256.219	197.316
M22	298.568	178.237	213.902	163.296
	263.921	162.243	196.841	147.420
M23	241.840	145.420	167.381	128.709
	230.237	130.744	150.026	116.802
M24	207.765	124.212	142.248	103.005
	196.626	111.833	124.954	99.225
M25	160.481	82.707	86.363	76.356
	152.703	76.295	78.936	71.442
M26	99.523	50.143	54.196	46.872
	94.767	43.932	48.441	43.848
M27	89.763	38.609	42.383	40.068
	84.781	33.861	36.349	37.044
M28	79.566	28.003	32.711	31.563
	74.040	22.995	24.874	27.594
M29	17.972	5.606	6.480	10.017
	0.000	0.000	0.000	0.000

The $^{40}Ar/^{39}Ar$ age of 124 ± 1 Ma obtained from reversely magnetized granitic plutons from Québec (Foland and others, 1986) may be correlative to CM3, or to the shorter duration CM0 or CM1. Ten major igneous complexes with $^{40}Ar/^{39}Ar$ ages tightly bunched around 124 Ma record only reversed polarity (Foster and Symons, 1979), and it seems likely that the reversed polarity chron is CM3 which has more than three times the duration of any reversed polarity chron in the younger part of the M-sequence. The duration of the interval between CM0 and CM3 is about 3.5 my, leading to an age for the base of CM0 of about 120.5 Ma.

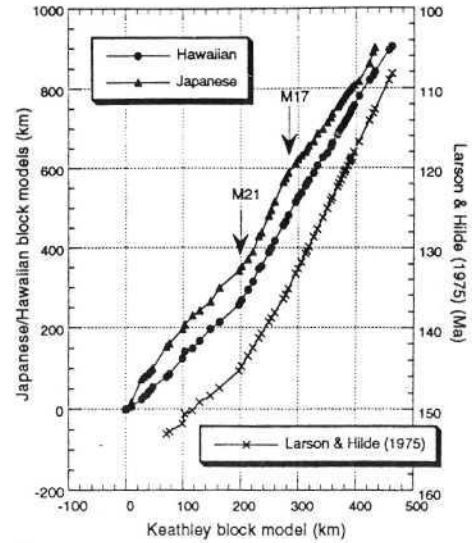

FIG. 6.—Block model distances from Japanese/Hawaiian lineations and Larson and Hilde (1975) block model plotted against Keathley block model distances.

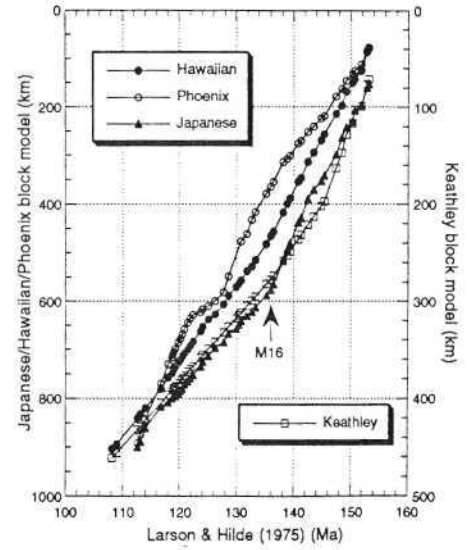

FIG. 7.—Japanese, Hawaiian, Phoenix and Keathley block model distances plotted against the Hawaiian block model of Larson and Hilde (1975).

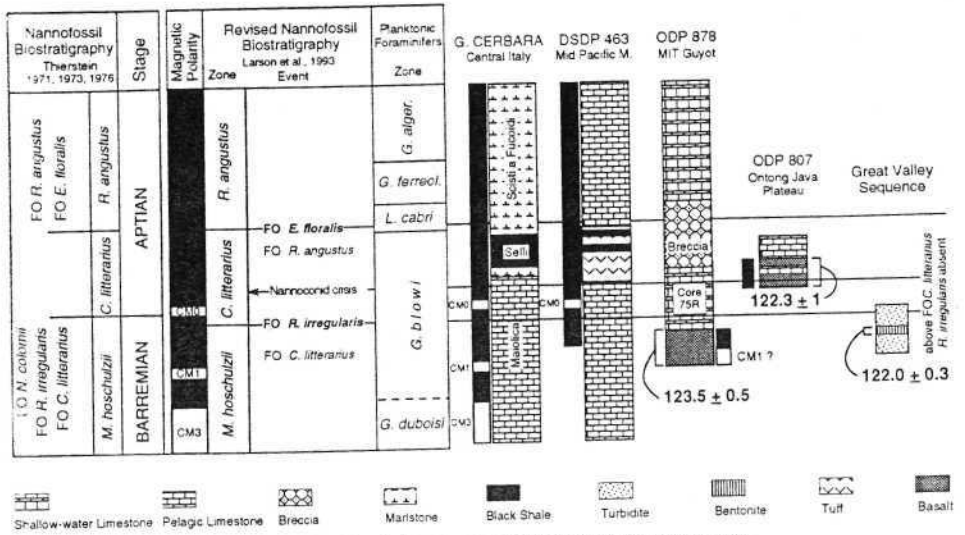

FIG. 8.—Stratigraphic and radiometric age control at the Barremian-Aptian boundary.

Duration estimates for the Aptian, Albian and Cenomanian stages have been obtained from lithologic cyclostratigraphy in Italian pelagic limestones (Herbert and others, this volume). These authors utilized the $^{40}Ar/^{39}Ar$ age estimate for the Cenomanian/Turonian boundary (93.5 ± 0.2 Ma) (Obradovich, 1993) and deduced an age of 122 Ma for the Barremian/Aptian boundary (base of CM0). Using similar reasoning based on cyclostratigraphic data (cited in Herbert and others, this volume), Obradovich (1993) arrived at an estimate of 121 Ma for this stage boundary.

A U-Pb zircon age estimate of 137.1 (+1.6/-0.6) Ma from the Great Valley Sequence of Northern California has been correlated to CM16 or CM16n (Bralower and others, 1990). This is an indirect correlation to the polarity time scale using nannofossil stratigraphy. The interval containing the two dated tuff layers was attributed to the Upper Berriasian *Assipetra infracretacea* subzone based on three nannofossil events: (1) the first occurrence (FO) of *Cretarhabdus angustiforatus* which was used to define the base of the *A. infracretacea* subzone, (2) the occurrence of *Rhagodiscus nebulosus* and (3) the absence of *Percivalia fenestrata*, the FO of which defines the top of the assigned subzone. Close inspection of the ranges of the three marker species suggests that the correlation of the two volcanic layers to CM16 or CM16n is too restrictive. Although *C. angustiforatus* was first observed at the base of Horizon A (Bralower and others, 1990), its FO cannot be placed at that level with certainty. Calcareous nannofossils are documented in only two samples in more than 40 m of section below Horizon A (Bralower and others, 1990) and *C. angustiforatus* generally has rare and scattered occurrence in the lower part of its range. For these reasons, we consider that the presence of *C. angustiforatus* indicates that this level is correlative to polarity chron CM16 or younger (Fig. 9) but does not provide further resolution. Bralower and others (1990) considered *R. nebulosus* to be restricted to the Upper Berriasian/Lower Valanginian interval. The FO of *R. nebulosus* ranges from CM17n to CM15 in sections where it has been correlated to polarity chrons (Fig. 9), but this species has been observed in very few sections. It has been observed in the lowermost Berriasian at Broyon, where it occurs below the *B. grandis* ammonite Zone and within the B calpionellid Zone (Bralower and others, 1989). The FO of *P. fenestrata* ranges from CM16n to CM14 (Fig. 9) and this species is generally rare and discontinuous in distribution. The correlation of this event to polarity CM14 has been observed at Fonte Giordano (Bralower and others, 1989); however, nannofossil perservation is very poor at this location. At Capriolo, the FO of *P. fenestrata* was observed within CM15n (Channell and others, 1987). An additional biostratigraphic constraint on the 137.1 Ma volcanic horizon is given by the absence of *Calcicalathina oblongata* (see Fig. 2 in Bralower and others, 1990); the FO has been correlated to CM14 and occasionally to CM13 (Fig. 9). If the absence of this species is considered as age diagnostic, then the 137.1 Ma datum is correlative to the CM16-CM15 interval (Fig. 9).

The age of 154 Ma for the young end of CM25 is based on the correlation of this polarity chron boundary to the Oxfordian/Kimmeridgian boundary (Ogg and others, 1984) and to age estimates for this stage boundary of about 154–156 Ma from California (Schweickert and others, 1984) and Oregon (Pessagno and Blome, 1990). In the Californian Sierra Nevada, the ammonite-bearing Mariposa Formation is a synorogenic flysch supposed to contain the Oxfordian/Kimmeridgian boundary

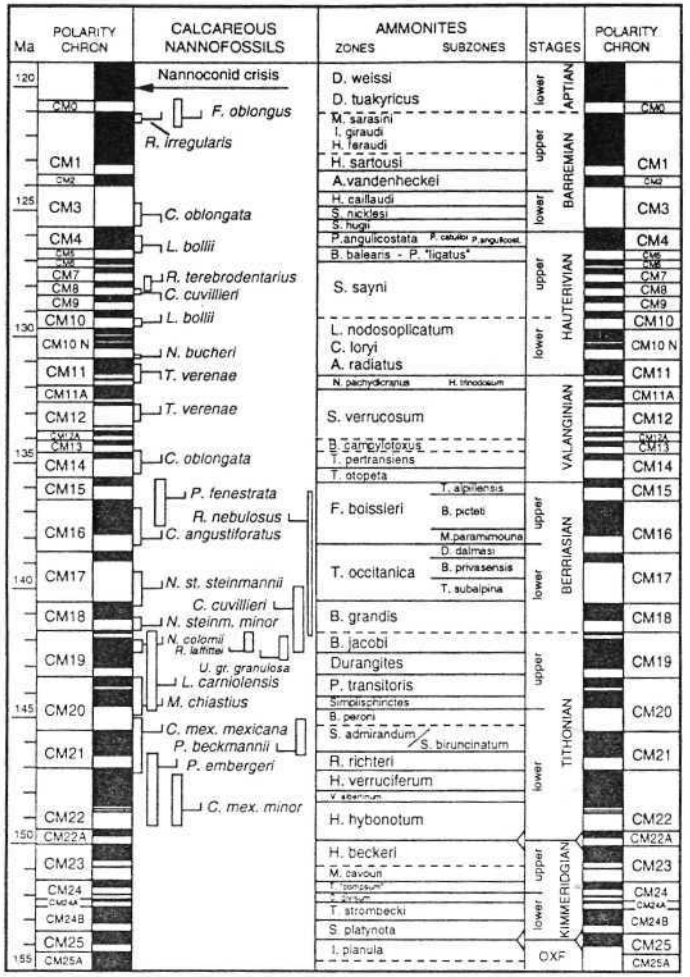

FIG. 9.—Stratigraphic framework for the Oxfordian to Aptian interval. Open bars indicate the range of the nannofossil events with respect to polarity chrons.

(Imlay, 1961) and is affected by Nevadan orogeny. K-Ar hornblende ages and U-Pb zircon ages on dykes and plutons appear to constrain the age of the Mariposa Formation and the Nevadan orogeny to the 154–159 Ma interval (see Schweickert and others, 1984) but many of the age determinations are not high quality by modern standards. More recent $^{40}Ar/^{39}Ar$ and concordant U/Pb zircon ages from the Klamath Mountains apparently constrain the Oxfordian/Kimmeridgian boundary to the 150–157 Ma interval (see Pessagno and Blome, 1990). The critical age determination is a concordant U-Pb age of 157 ± 1.5 Ma (Saleeby, 1984; Harper and others, 1994) underlying a macrofossil assemblage correlated to the middle and upper Oxfordian interval (Imlay, 1980). This age determination correlates to the overlapping occurrence of radiolaria *Mirifusus* and *Xiphostylus*, considered to mark the middle-upper Oxfordian interval in the Klamath Mountains (Pessagno and Blome, 1990), however, this is controversial as *Mirifusus* and *Xiphostylus* are both present from Aalenian time in Mediterranean sections (see Baumgartner, 1987). A 154 Ma age for M25 is consistent with a K-Ar age of 155 ± 3.4 Ma from a celadonite vein

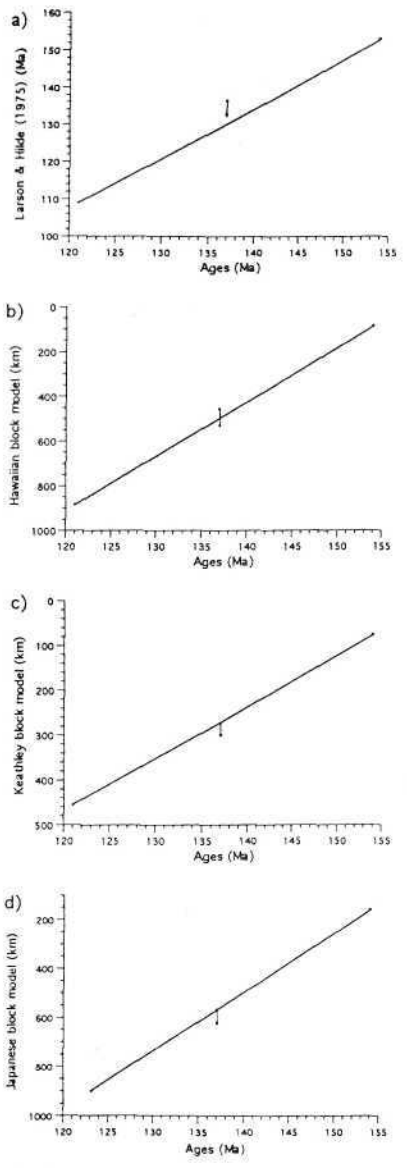

FIG. 10.—The selected radiometric age determinations for M0 (121 Ma), M16-M15 (137 Ma) and M25 (154 Ma) plotted against (a) the Larson and Hilde (1975) block model, (b) Hawaiian block model, (c) Keathley block model, (d) Japanese block model. M0 is not present in the Japanese lineations (Table 2) and for (d) the young end of M1 is assigned an age of 123.2 Ma.

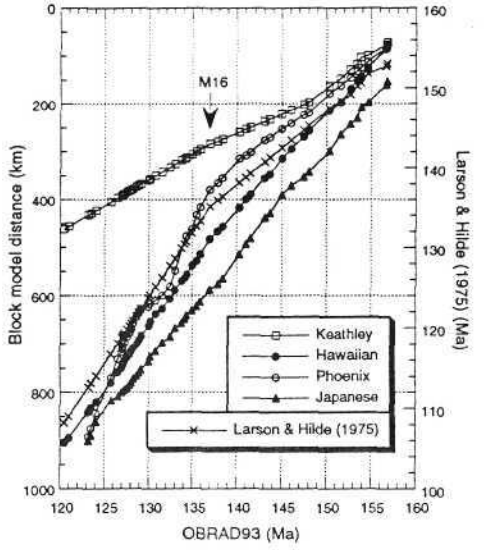

FIG. 11.—OBRAD93 time scale (Obradovich, 1993) compared to oceanic magnetic anomaly block models.

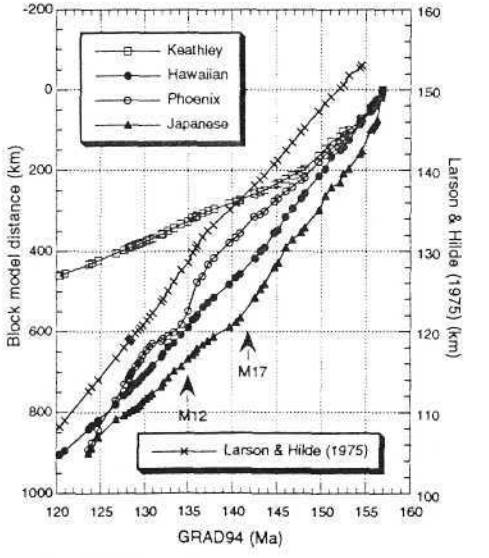

FIG. 12.—GRAD94 time scale (Gradstein and others, 1994, this volume) compared to oceanic magnetic anomaly block models.

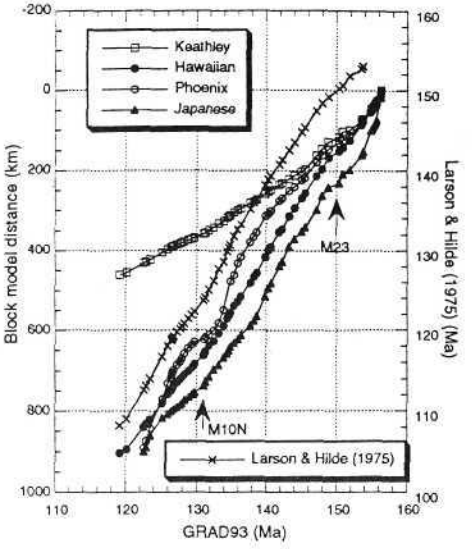

FIG. 13.—GRAD93 time scale (Gradstein and others, this volume) compared to oceanic magnetic anomaly block models.

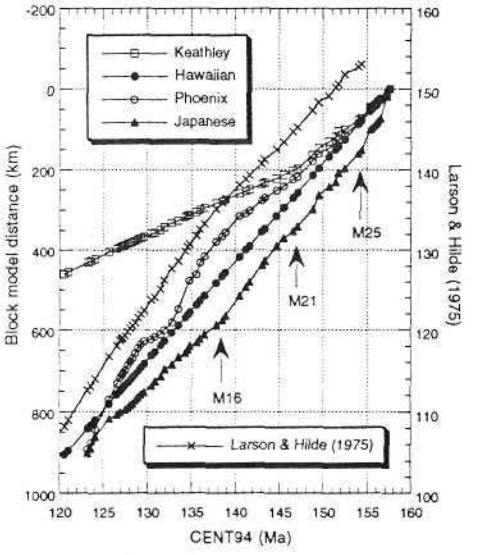

FIG. 14.—CENT94 time scale (this paper) compared to oceanic magnetic anomaly block models.

TABLE 3.—TIME SCALES FOR THE M0-M25 AND M0-M29 INTERVALS. LH75 (LARSON AND HILDE, 1975), KG85 (KENT AND GRADSTEIN, 1985), GTS89 (HARLAND AND OTHERS, 1990), GRAD93 AND GRAD94 (GRADSTEIN AND OTHERS, 1994, THIS VOLUME), CENT94 (THIS PAPER). POLARITY CHRON NOMENCLATURE AFTER HARLAND AND OTHERS (1982).

Reversed Chron	LH75 (Ma)	KG85 (Ma)	GTS89 (Ma)	GRAD93 (Ma)	GRAD94 (Ma)	CENT94 (Ma)
M0 (top)	108.19	118.00	124.32	119.15	120.38	120.60
(base)	109.01	118.70	124.88	120.10	120.98	121.00
M1	112.62	121.81	127.35	122.56	123.67	123.19
	113.14	122.25	127.70	122.88	124.04	123.55
M3	114.05	123.03	128.32	123.45	124.72	124.05
	116.75	125.36	130.17	125.15	126.73	125.67
M5	118.03	126.46	131.05	125.96	127.68	126.57
	118.72	127.05	131.51	126.39	128.19	126.91
M6	118.91	127.21	131.64	126.50	128.33	127.11
	119.06	127.34	131.74	126.60	128.44	127.23
M7	119.27	127.52	131.89	126.80	128.59	127.49
	119.79	127.97	132.25	127.25	128.98	127.79
M8	120.21	128.33	132.53	127.68	129.29	128.07
	120.52	128.60	132.75	127.98	129.53	128.34
M9	120.88	128.91	132.99	128.32	129.79	128.62
	121.49	129.43	133.41	128.88	130.24	128.93
M10	121.94	129.82	133.72	129.31	130.58	129.25
	122.37	130.19	134.01	129.71	130.90	129.63
M10Nn-1	122.82	130.57	134.31	130.13	131.23	129.91
	122.88	130.63	134.36	130.20	131.28	129.95
M10Nn-2	123.31	131.00	134.65	130.60	131.60	130.22
	123.34	131.02	134.67	130.62	131.62	130.24
M10N	123.73	131.36	134.94	130.99	131.91	130.49
	124.07	131.65	135.17	131.26	132.10	130.84
M11	125.10	132.53	135.87	131.81	132.70	131.50
	125.68	133.03	136.27	132.12	133.05	131.71
M11	125.74	133.08	136.31	132.15	133.08	131.73
	126.22	133.50	136.64	132.42	133.37	131.91
M11An-1				132.66	133.64	132.35
				132.68	133.66	132.40
M11A	127.16	134.01	137.30	132.92	133.93	132.47
	127.29	134.42	137.37	132.99	134.00	132.55
M12.1	127.68	134.75	137.63	133.19	134.23	132.76
	128.62	135.56	138.28	133.70	134.79	133.51
M12.2	128.74	135.66	138.36	133.75	134.85	133.58
	128.99	135.88	138.53	133.90	135.01	133.73
M12A	129.41	136.24	138.82	134.12	135.25	133.99
	129.56	136.37	138.92	134.20	135.34	134.08
M13	129.87	136.64	139.14	134.37	135.53	134.27
	130.41	137.10	139.50	134.66	135.84	134.53
M14	130.75	137.39	139.73	134.84	136.04	134.81
	131.81	138.30	140.46	135.41	136.67	135.57
M15	132.63	139.01	141.02	135.90	137.21	135.96
	133.30	139.58	141.47	136.38	137.89	136.49
M16	135.18	141.20	142.76	137.72	139.68	137.85
	135.94	141.85	143.28	138.26	140.40	138.50
M17	136.42	142.27	143.61	138.51	140.86	138.89
	138.16	143.76	144.80	139.86	142.51	140.51
M18	138.82	144.33	145.25	140.33	143.14	141.22
	139.31	144.75	145.58	140.68	143.60	141.63
M19n-1	139.46	144.88	145.69	140.80	143.72	141.78
	139.55	144.96	145.75	140.88	143.79	141.88
M19	140.74	145.98	146.56	141.82	144.68	143.07
	141.28	146.44	146.93	142.25	145.08	143.36
M20n-1	141.64	146.75	147.17	142.54	145.35	143.77
	141.71	146.81	147.22	142.60	145.41	143.84
M20	142.47	147.47	147.75	143.21	145.99	144.70
	143.47	148.33	148.43	144.01	146.74	145.52
M21	144.74	149.42	149.30	145.02	147.69	146.56
	145.29	149.89	149.67	145.46	148.11	147.06
M22n-1	147.11	151.46	150.92	146.92	149.48	148.57
	147.17	151.51	150.96	146.95	149.52	148.62
M22n-2	147.23	151.56	151.00	147.01	149.57	148.67
	147.29	151.61	151.04	147.06	149.61	148.72
M22	147.38	151.69	151.10	147.13	149.68	148.79
	148.36	152.53	151.77	147.91	150.42	149.49
M22A	148.51	152.66	151.87	148.03	150.53	149.72
	148.72	152.84	152.01	148.20	150.69	150.04
M23	149.15	153.21	152.31	148.50	151.00	150.69
	149.48	153.49	152.53	149.24	151.39	150.91
M23	149.51	153.52	152.56	149.30	151.42	150.93
	150.24	154.15	153.06	150.31	152.10	151.40
M24	150.63	154.48	153.32	150.85	152.46	151.72
	151.06	154.85	153.61	151.44	152.86	151.98

TABLE 3.—*Continued*

Reversed Chron	LH75 (Ma)	KG85 (Ma)	GTS89 (Ma)	GRAD93 (Ma)	GRAD94 (Ma)	CENT94 (Ma)
M24	151.09	154.88	153.64	151.49	152.89	152.00
	151.33	155.08	153.80	151.82	153.11	152.15
M24A	151.48	155.21	153.90	152.02	153.25	152.24
	151.79	155.48	154.11	152.46	153.54	152.43
M24B	152.21	155.84	154.40	153.04	153.93	153.13
	152.39	156.00	154.53	153.30	154.10	153.43
M25	152.73	156.29	154.76	153.52	154.31	154.00
	153.03	156.55	154.96	153.72	154.49	154.31
M26					155.51	155.32
					155.69	155.55
M27					155.83	155.80
					156.00	156.05
M28					156.14	156.19
					156.29	156.51
M29					156.77	157.27
					156.85	157.53

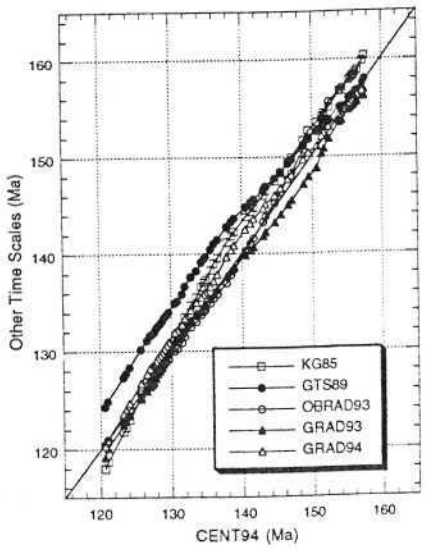

FIG. 15.—Plot of various time scales against CENT94. LH75 (Larson and Hilde, 1975); KG85 (Kent and Gradstein, 1985); GTS89 (Harland and others, 1990); GRAD93 and GRAD94 (Gradstein and others, 1994, this volume); CENT94 (this paper).

(Ludden, 1992) in basaltic crust from the Argo Abyssal Plain (ODP Site 765) which lies between oceanic magnetic anomalies interpreted as M26 and M25A (Sager and others, 1992).

A REVISED TIME SCALE BASED ON THE NEW HAWAIIAN BLOCK MODEL

The three age estimates discussed above for the base of CM0 (121 Ma), CM16-CM15 (137 Ma) and the top CM25 (154 Ma) are similar to the polarity chron age estimates adopted in other recent time scales (e.g., Obradovich, 1993). These age estimates are not consistent with constant spreading rate in LH75 (Fig. 10A); they are consistent with constant spreading in the new Hawaiian block model (Fig. 10B) and marginally consistent with constant spreading in the Keathley and Japanese block models (Figs. 10C, D).

In OBRAD93 (Obradovich, 1993), the Early Cretaceous time scale is constructed by interpolation using LH75 between three tie points: base CM0 at 121 Ma, CM16/CM16n chron boundary at 137 Ma, and CM25n at 156 Ma. This implies an abrupt change in spreading rate at 137 Ma in LH75 and other block models (Fig. 11). GRAD94 implies constant spreading rate for most of LH75, with a spreading rate change in the M12-M17 interval (Fig. 12). For GRAD94, base CM0 is at 120.98 Ma, 137 Ma lies in CM15n, and top CM25 is at 154.3 Ma, consistent with the popular age estimates cited above. For GRAD93 (Fig. 13), inflexions in the distance-time plots at about 130 Ma (M10N) at about 150 Ma (M23) for the Hawaiian, Japanese and Keathley records appear to be an artifact of the GRAD93.

As mentioned above, the method used to construct the new Hawaiian block model, although optimal for determining the bounds of the principal anomalies, does not allow the minor anomalies to be incorporated in the block model (Fig. 4, Table 2). For the minor polarity chrons, we adopt the relative position within the individual major polarity chron from LH75. In our time scale based on the new Hawaiian block model (CENT94), the only modification to the number of polarity chrons in LH75 is the inclusion of an additional reversed polarity chron (CM11An-1, Table 3). This results in two reversed polarity chrons between CM11 and CM12, as proposed by Tamaki and Larson (1988). The two reversed polarity chrons between CM11 and CM12 were recognized in the Capriolo land section (Channell and others, 1987) at 24–34% and 42–48% (from the base) of the normal polarity zone between CM11 and CM12. We adopt this spacing of the two reversed polarity chrons.

The resulting time scale (CENT94) implies a spreading rate decrease for M16-M25 in the LH75 block model, and an increase in spreading rate for M21-M29 time (148–157 Ma) in the Keathley block model (Fig. 14). CENT94 implies a spreading rate increase for M16-M29 (139–157 Ma) in the Japanese block model and variable spreading rates in the Phoenix block model (Fig. 14). Figure 15 illustrates the relationship between CENT94 and other time scales.

Cyclostratigraphy permits polarity chron duration to be estimated where Milankovitch-type cycles can be documented and provides a potential means of testing time scales such as GTS89, GRAD94 and the new time scale based on the new Hawaiian block model (CENT94). For two sections in the underlying Maiolica Limestones (Gorgo a Cerbara and Cismon) which record polarity zones correlative to CM0-CM3, bedding rhythms appear to record both the eccentricity and precession periodicities (Herbert, 1992). The durations of CM0-CM3 in CENT94 are generally lower than predicted from the cyclostratigraphy (Fig. 16).

CORRELATION OF STAGE BOUNDARIES TO THE POLARITY TIME SCALE

In the past 15 years, Cretaceous polarity chrons have been correlated with calpionellid, nannofossil and foraminiferal events in numerous pelagic limestone sections from Southern Alps, Central Italy, Atlantic and Pacific oceans, although poor

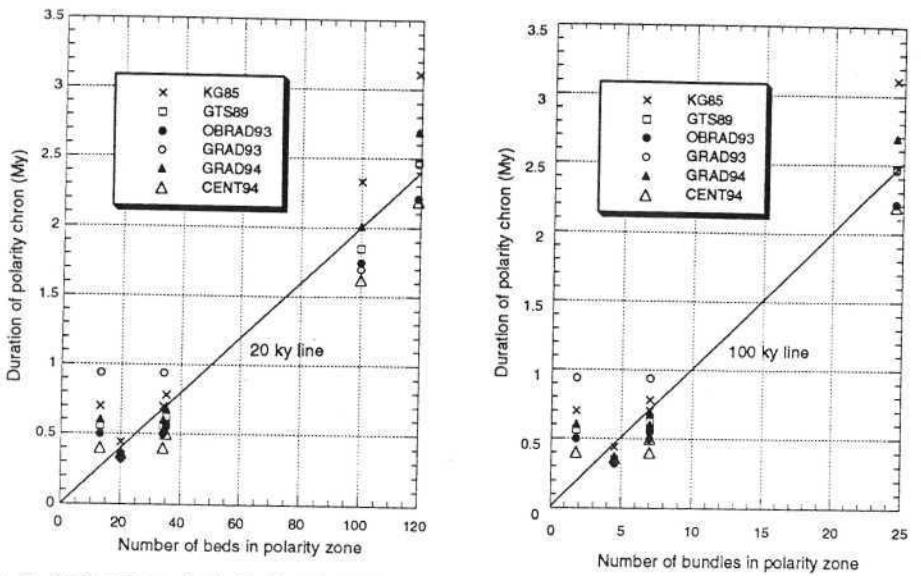

FIG. 16.—Numbers of beds and bedding bundles within individual polarity chrons (after Herbert, 1992) plotted against polarity chron duration according to various time scales. KG85 (Kent and Gradstein, 1985), GTS89 (Harland and others, 1990), GRAD93 and GRAD94 (Gradstein and others, 1994, this volume), OBRAD93 (Obradovich, 1993), CENT94 (this paper).

TABLE 4.—LATE JURASSIC-EARLY CRETACEOUS STAGE BOUNDARY AGES. GTS82 (HARLAND AND OTHERS, 1982); KG85 (KENT AND GRADSTEIN, 1985); GTS89 (HARLAND AND OTHERS, 1990); OBRAD93 (OBRADOVICH, 1993); GRAD93 AND GRAD94 (GRADSTEIN AND OTHERS, 1994, THIS VOLUME); CENT94 (THIS PAPER)

Stage Boundary	GTS82 (Ma)	KG85 (Ma)	GTS89 (Ma)	OBRAD93 (Ma)	GRAD93 (Ma)	GRAD94 (Ma)	CENT94 (Ma)
Barr.-Apt.	119	119	124.5	121	119.0	121.0 ± 1.4	121.0
Haut.-Barr.	125	124	131.8	127	127.3	127.0 ± 1.6	126.0
Val.-Haut.	131	131	135.0	130	131.6	132.0 ± 1.9	131.5
Berr.-Val.	138	138	140.7	135	138.8	137.0 ± 2.2	135.8
Tith.-Berr.	144	144	145.6	142	144.8	144.2 ± 2.6	141.6
Kimm.-Tith.	150	152	152.1		152.8	150.7 ± 3.0	150.0
Oxf.-Kimm.	156	156	154.7			154.1 ± 3.2	154.0

to moderate preservation of nannoflora accounts for some variability in their correlation (Fig. 9). Late Jurassic and Cretaceous chronostratigraphy is based on stage stratotypes defined by ammonite zones. Due to absence or uneven distribution of ammonite faunas in land sections and oceanic cores, correlation of Cretaceous stage boundaries to polarity chrons has been based on the supposed correlation of calcareous microplankton events to ammonites (e.g., Thierstein, 1973). In the last few years, ammonite biozones have been directly correlated to magnetostratigraphy in parts of the Oxfordian-lowermost Valanginian (see Ogg and others, 1991) and Valanginian-Barremian intervals (Cecca and others, 1994; Channell and others, 1994).

The Oxfordian/Kimmeridgian boundary is correlative to the base of the *Sutneria platynota* ammonite Zone which has been correlated to CM25 in southern Spain (Ogg and others, 1984). The Kimmeridgian/Tithonian boundary is correlative to the base of the *Hybonoticeras hybonotum* ammonite Zone which lies close to CM22A also in southern Spain (Ogg and others, 1984). The Tithonian/Berriasian (Jurassic/Cretaceous) boundary does not have a universally accepted definition. Many of the candidate markers have been correlated to the polarity chrons (Ogg and Lowrie, 1986; Channell and Grandesso, 1987; Bralower and others, 1989; Ogg and others, 1991). The base of CM18 (top of *Berriasella jacobi* ammonite Zone) has become the generally accepted correlation to the Tithonian-Berriasian boundary. The Berriasian/Valanginian boundary is defined by the base of the *T. otopeta* ammonite Zone, and falls within CM15n (Ogg and others, 1988) and between the FO of *Cretarhabdus angustiforatus* and the FO of *Calcicalathina oblongata*. The Valanginian/Hauterivian boundary coincides with the base of the *A. radiatus* ammonite Zone and correlates to the base of CM11n (Channell and others, 1994). The base of the *Spitidiscus hugii* ammonite Zone defines the Hauterivian/Barremian boundary, which falls between the LO of *Lihtraphidites bollii*

and the LO of *Calcicalathina oblongata*, and in the upper part of CM4 (Cecca and others, 1994). The Barremian/Aptian boundary was formally defined at the first occurrence of *Deshayesites*. None of the nannofossil events proposed by Thierstein (1973) to define this boundary have proved to be reliable. The FO of *Rucinolithus irregularis* is correlated to the upper part of the *M. sarasini* ammonite Zone and is therefore slightly older than the Barremian/Aptian boundary (Channell and Erba, 1992, Coccioni and others, 1992). The base of CM0 coincides closely to this boundary. Direct correlation of this polarity chron with ammonite biozones has not been well documented, although a single specimen of *Prodeshayesites* sp. occurs near the top of CM0 at Gorgo a Cerbara indicating that at least part of this polarity chron is Early Aptian in age (Channell and others, 1994). The correlation of polarity chrons to ammonite zones in the Early Cretaceous (Fig. 9) indicates substantial variation in duration of ammonite zones.

CONCLUSIONS

Although considerable progress has been made in the correlation of paleontological events and biozones to the M-sequence polarity chrons, the absolute age control on the Late Jurassic-Early Cretaceous time scale remains poor. We consider that the available absolute age control is insufficient to justify abandoning the constant oceanic spreading rate assumption for this part of the time scale. Comparison of block models from Japanese, Hawaiian, Phoenix and Keathley lineations indicates that the Hawaiian record is closest to a constant spreading rate record. The new Hawaiian block model differs slightly from that published by Larson and Hilde (1975). The absolute ages for CM0 (121 Ma), CM16-M15 (137 Ma) and CM25 (154 Ma) are considered to be the only reliable estimates for M-sequence polarity chrons, and these ages are consistent with constant spreading in the new Hawaiian block model.

The resulting time scale (CENT94) based on the new Hawaiian block model yields the following stage boundary ages: Barremian/Aptian (121 Ma), Hauterivian/Barremian (126 Ma), Valanginian/Hauterivian (131.5 Ma), Berriasian/Valanginian (135.8 Ma), Tithonian/Berriasian (141.6 Ma), Kimmeridgian/Tithonian (150 Ma), Oxfordian/Kimmeridgian (154 Ma). See Figure 15, Table 3 and Table 4 for comparisons among published time scales.

ACKNOWLEDGMENTS

We are grateful to Tim Bralower, Tim Herbert, Roger Larson and Neil Opdyke for reviews of an early draft of this manuscript, and to Malcolm Pringle for discussions. J. C. acknowledges financial support from the United States National Science Foundation (OCE 8915697).

REFERENCES

BAUMGARTNER, P. O., 1987, Age and genesis of Tethyan Jurassic radiolarites: Eclogae Geologicae Helvetiae, v. 80, p. 831–879.

BRALOWER, T. J., MONECHI, S., AND THIERSTEIN, H. R., 1989, Calcareous nannofossil zonation of the Jurassic-Cretaceous boundary interval and correlation with the geomagnetic polarity timescale: Marine Micropaleontology, v. 14, p. 153–235.

BRALOWER, T. J., LUDWIG, K. R., OBRADOVICH, J. D., AND JONES, D. L., 1990, Berriasian (Early Cretaceous) radiometric ages from the Grindstone Creek Section, Sacramento Valley, California: Earth and Planetary Science Letters, v. 98, p. 62–73.

CECCA, F., PALLINI, G., ERBA, E., PREMOLI-SILVA, I., AND COCCIONI, R., 1994, Hauterivian-Barremian chronostratigraphy based on ammonites, nannofossils, planktonic foraminifera and magnetic chrons from the Mediterranean domain: Cretaceous Research, v. 15, p. 457–467.

CHANNELL, J. E. T., BRALOWER, T. J., AND GRANDESSO, P., 1987, Biostratigraphic correlation of Mesozoic polarity chrons CM1 to CM23 at Capriolo and Xausa (Southern Alps, Italy): Earth and Planetary Science Letters, v. 85, p. 203–221.

CHANNELL, J. E. T., CECCA, F., AND ERBA, E., 1994, Correlations of Hauterivian and Barremian (Early Cretaceous) stage boundaries to polarity chrons: Transactions American Geophysical Union (EOS), v. 75, p. 202.

CHANNELL, J. E. T. AND ERBA, E., 1992, Early Cretaceous polarity chrons CM0 to CM11 recorded in Northern Italian land sections near Brescia (Northern Italy): Earth and Planetary Science Letters, v. 108, p. 161–179.

CHANNELL, J. E. T. AND GRANDESSO, P., 1987, A revised correlation of Mesozoic polarity chrons and calpionellid zones: Earth and Planetary Science Letters, v. 85, p. 222–240.

COCCIONI, R., ERBA, E., AND PREMOLI SILVA, I., 1992, Barremian-Aptian calcareous plankton biostratigraphy from the Gorgo Cerbara section (Marche, central Italy) and implications for plankton evolution: Cretaceous Research, v. 13, p. 517–537.

COLEMAN, D. S. AND BRALOWER, T. J., 1993, New U-Pb zircon age constraints on the Early Cretaceous time scale: Transactions American Geophysical Union (EOS), v. 73, p. 556.

FOLAND, K. A., GILBERT, L. A., SEBRING, C. A., AND JIANG-FENG, C., 1986, $^{40}Ar/^{39}Ar$ ages for plutons of the Monteregian Hills, Quebec: evidence for a single episode of Cretaceous magmatism: Geological Society America Bulletin, v. 97, p. 966–974.

FOSTER, J. AND SYMONS, D. T. A., 1979, Defining a paleomagnetic polarity pattern in the Monteregian intrusives: Canadian Journal of Earth Sciences, v. 16, p. 1716–1725.

GRADSTEIN, F. M., AGTERBERG, F. P., OGG, J. G., HARDENBOL, J., VAN VEEN, P., THIERRY, J., AND HUANG, Z., 1994, A Mesozoic time scale: Journal of Geophysical Research, v. 99, p. 24,051–24,074.

HARLAND, W. B., COX, A. V., LLEWELLYN, P. G., PICKTON, C. A. G., SMITH, A. G., AND WALTERS, R., 1982, A Geologic Time Scale: Cambridge, Cambridge University Press, 131 p.

HARLAND, W. B., ARMSTRONG, R. L., COX, A. V., CRAIG, L. E., SMITH, A. G. AND SMITH, D. G., 1990, A Geologic Time Scale: Cambridge, Cambridge University Press, 263 p.

HARPER, G. D., SALEEBY, J. B., AND HEIZLER, M., 1994, Formation and emplacement of the Josephine ophiolite and the Nevadan orogeny in the Klamath Mountains, California-Oregon: U/Pb zircon and 40Ar/39Ar geochronology: Journal of Geophysical Research, v. 99, p. 4293–4321.

HERBERT, T. D., 1992, Paleomagnetic calibration of Milankovitch cyclicity in Lower Cretaceous sediments: Earth and Planetary Science Letters, v. 112, p. 15–28.

IMLAY, R. W., 1961, Late Jurassic ammonites from the western Sierra Nevada, California: Washington, D.C., United States Geological Survey Professional Paper 374D, p. D1–D30.

IMLAY, R. W., 1980, Jurassic paleobiogeography of the western conterminous United states in its continental setting: Washington, D.C., United States Geological Survey Professional Paper 1062, 134 p.

KENT, D. V. AND GRADSTEIN, F. M., 1985, A Cretaceous and Jurassic geochronology: Geological Society of America Bulletin, v. 96, p. 1419–1427.

KLITGORD, K. D. AND SCHOUTEN, H., 1986, Plate kinematic of the central Atlantic, *in* Vogt, P. R. and Tucholke, B. E., eds., The Geology of North America, The Western North Atlantic Region, v. M: Boulder, Geological Society of America, p. 351–378.

LARSON, R. L., FISCHER, A. G., ERBA, E., AND PREMOLI SILVA, I., eds., 1993, APTICORE-ALBICORE: A Workshop Report on Global Events and Rhythms of the mid-Cretaceous, 4–9 October 1992, Perugia, Italy: Washington, D.C., Joint Oceanographic Institutions Inc., 56 p.

LARSON, R. L. AND HILDE, T. W. C., 1975, A revised time scale of magnetic reversals for the Early Cretaceous and Late Jurassic: Journal of Geophysical Research, v. 80, p. 2586–2594.

LUDDEN, J. N., 1992, Radiometric age determinations for basement from sites 765 and 766, Argo Abyssal Plain and northwestern Australian margin, *in* Gradstein, F. M., Ludden, J. N., and others, eds., Proceedings of Ocean Drilling Program, Scientific Results 123: College Station, Ocean Drilling Program, p. 557–559.

MAHONEY, J. J., STOREY, M., DUNCAN, R., SPENCER, K. J., AND PRINGLE, M., 1993, Geochemistry and age of the Ontong-Java Plateau, *in* Pringle, M. S., Sager, W. W., Sliter W. V., and Stein, S., eds., Monograph on the Mesozoic Pacific: Washington, D.C., American Geophysical Union, p. 233–261.

NAKANISHI, M., TAMAKI, K., AND KOBAYASHI, K., 1989, Mesozoic magnetic anomaly lineations and seafloor spreading history of the northwestern Pacific: Journal of Geophysical Research, v. 94, p. 15437–15462.

NAKANISHI, M., TAMAKI, K., AND KOBAYASHI, K., 1992, Magnetic anomaly lineations from Late Jurassic to Early Cretaceous in the west-central Pacific Ocean: Geophysical Journal International, v. 109, p. 701–719.

OBRADOVICH, J. D., 1993, A Cretaceous time scale, *in* Caldwell, W. G. E., ed., Evolution of the Western Interior Basin: St. Johns, Geological Association of Canada Special Paper 39, p. 379–396.

OGG, J. G., COMPANY, M., STEINER, M. B., AND TAVERA, J. M., 1988, Magnetostratigraphy across the Berriasian-Valanginian boundary (Early Cretaceous) at Cehegin (Murcia Province, southern Spain): Earth and Planetary Science Letters, v. 87, p. 205–215.

OGG, J. G., HASENYAGER, R. W., WIMBLEDON, W. A., CHANNELL, J. E. T., AND BRALOWER, T. J., 1991, Magnetostratigraphy of the Jurassic-Cretaceous boundary interval—Tethyan and English faunal realms: Cretaceous Research, v. 12, p. 455–482.

OGG, J. G. AND LOWRIE, W., 1986, Magnetostratigraphy of the Jurassic/Cretaceous boundary: Geology, v. 14, p. 547–550.

OGG, J. G., STEINER, M. B., OLORIZ, F., AND TAVERA, J. M., 1984, Jurassic magnetostratigraphy: 1. Kimmeridgian-Tithonian of Sierra Gorda and Carcabuey, southern Spain: Earth and Planetary Science Letters, v. 71, p. 147–162.

PESSAGNO, E. A. AND BLOME, C. D., 1990, Implications of new Jurassic stratigraphic, geochrononometric and paleolatitudinal data from the western Klamath terrane (Smith River and Rogue Valley subterranes): Geology, v. 18, p. 665–668.

PRINGLE, M. S., STAUDIGEL, H., DUNCAN, R. A., CHRISTIE, D. M., ODP LEG 143 AND 144 SCIENTIFIC STAFFS, 1993, 40Ar/39Ar ages of basement lavas at Resolution, MIT, and Wodejebato Guyots compared with magneto- and bio-stratigraphic results from ODP Legs 143/144: Transactions American Geophysical Union (EOS), v. 73, p. 353.

SAGER, W. W., FULLERTON, L. G., BUFFLER, R. T., AND HANDSCHUMACHER, D. W., 1992, Argo Abyssal Plain magnetic lineations revisited: implications for the onset of seafloor spreading and tectonic evolution of the eastern Indian ocean, *in* Gradstein, F. M., Ludden, J. N., and others, eds., Proceedings of Ocean Drilling Program, Scientific Results 123: College Station, Ocean Drilling Program, p. 659–669.

SALEEBY, J. B., 1984, Pb/U zircon ages from the Rogue River area, western Jurassic belt, Klamath Mountains, Oregon: Geological Society America Abstracts with Programs, v. 16, p. 331.

SCHOLTEN, H. AND MCCAMY, K., 1972, Filtering marine magnetic anomalies: Journal of Geophysical Research, v. 77, p. 7089–7099.

SCHWEICKERT, R. A., BOGEN, A., GIRTY, N. L., HANSON, R. E., AND MERGUERIAN, C., 1984, Timing and structural expression of the Nevadan orogeny, Sierra Nevada, California: Geological Society of America Bulletin, v. 95, p. 967–979.

SLITER, W. V., 1992, Biostratigraphic zonation for Cretaceous planktonic foraminifers examined in thin section: Journal of Foraminiferal Research, v. 19, p. 1–19.

SUNDVIK, M. T. AND LARSON, R. L., 1988, Seafloor spreading history of the western North Atlantic Basin derived from the Keathley sequence and computer graphics: Tectonophysics, v. 155, p. 49–71.

TAMAKI, K. AND LARSON, R. L., 1988, The Mesozoic tectonic history of the Magellan microplate in the western central Pacific: Journal of Geophysical Research, v. 93, p. 2857–2874.

TARDUNO, J. A., SLITER, W. V., KROENKE, L., LECKIE, M., MAYER, H., MAHONEY, J. J., MUSGRAVE, R., STOREY, M., AND WINTERER, E. L., 1991, Rapid formation of the Ontong Java Plateau by Aptian mantle plume volcanism: Science, v. 254, p. 399–403.

THIERSTEIN, H. R., 1971, Tentative Lower Cretaceous calcareous nannoplankton zonation: Eclogae Geologicae Helvetiae, v. 64, p. 459–488.

THIERSTEIN, H. R., 1973, Lower Cretaceous calcareous nannoplankton biostratigraphy: Abhandlungen der Geologischen Bundesanstalt, v. A 29, p. 1–52.

THIERSTEIN, H. R., 1976, Mesozoic calcareous nannoplankton biostratigraphy of marine sediments: Marine Micropaleontology, v. 1, p. 325–362.

WESSEL, P. AND SMITH, W. H., 1991, Free software helps map and display data: Transactions American Geophysical Union (EOS), v. 72, p. 441–446.